



## Thyroxine and reserpine-induced changes in metabolic profiles of rat urine and the therapeutic effect of Liu Wei Di Huang Wan detected by UPLC-HDMS

Ping Wang, Hui Sun, Haitao Lv, Wenjun Sun, Ye Yuan, Ying Han, Dongwu Wang, Aihua Zhang, Xijun Wang\*

National TCM Key Lab of Serum Pharmacochimistry, Heilongjiang University of Chinese Medicine, Heping Road 24, Harbin 150040, China

### ARTICLE INFO

#### Article history:

Received 26 February 2010  
Received in revised form 25 April 2010  
Accepted 26 April 2010  
Available online 4 May 2010

#### Keywords:

Metabonomics  
UPLC-HDMS  
Liu Wei Di Huang Wan  
Kidney yin deficiency

### ABSTRACT

The promise of metabonomics, a new “omics” technique, to validate Chinese medicines and the compatibility of Chinese formulas has been appreciated. The present study was undertaken to explore the excretion pattern of low molecular mass metabolites in the male Wistar-derived rat model of kidney yin deficiency induced with thyroxine and reserpine as well as the therapeutic effect of Liu Wei Di Huang Wan (LW) and its separated prescriptions, a classic traditional Chinese medicine formula for treating kidney yin deficiency in China. The study utilized ultra-performance liquid chromatography/electrospray ionization synapt high definition mass spectrometry (UPLC/ESI-SYNAPT-HDMS) in both negative and positive electrospray ionization (ESI). At the same time, blood biochemistry was examined to identify specific changes in the kidney yin deficiency. Distinct changes in the pattern of metabolites, as a result of daily administration of thyroxine and reserpine, were observed by UPLC-HDMS combined with a principal component analysis (PCA). The changes in metabolic profiling were restored to their baseline values after treatment with LW according to the PCA score plots. Altogether, the current metabonomic approach based on UPLC-HDMS and orthogonal projection to latent structures discriminate analysis (OPLS-DA) indicated 20 ions (14 in the negative mode, 8 in the positive mode, and 2 in both) as “differentiating metabolites”.

Crown Copyright © 2010 Published by Elsevier B.V. All rights reserved.

### 1. Introduction

Metabonomics, a scientific platform for investigating drug toxicity and gene function, is a new “omics” science in the post-genomics era that analyzes changes in the metabolic profile in both biofluids and tissues to explore global biologic states and gene regulation. The primary definition of metabonomics, as “the quantitative measurement of the dynamic multiparametric metabolic response of living systems to pathophysiological stimuli or genetic modification” [1], has recently demonstrated significant potential in many fields such as toxicity evaluation, disease diagnosis, drug discovery and plant genotype discrimination [2–4]. Metabolic responses of living systems lead to alterations of low molecular mass metabolites, thus changing the metabolic profile, such as the presence or concentrations of metabolites. To get as much information as possible, several analytical techniques have been employed. To date, NMR, which can provide high selectivity for all compounds, is the most popular technology used in metabonomics research [5].

Gas chromatography–mass spectrometry (GC–MS) is also widely used in metabonomics research but only for volatile components of the metabolites in biofluids and tissues [6]. However, most low molecular mass metabolites are non-volatile, so liquid chromatography coupled with mass spectrometry (LC–MS) as profiling tool has burgeoned [7]. Following the appearance of Ultra-Performance Liquid Chromatography (UPLC), developed by the Waters Company in 2005, minor particles (sub 1.7  $\mu\text{m}$ ) have greatly improved the resolution, sensitivity and analytical speed, integrating with Q-TOF-HDMS to form a new high-performance scientific platform for metabonomics research [2,8]. As a new “omics” technique, the application prospect of metabonomics in the activity validation of Chinese medicines and natural active constituent discovery has been appreciated. Its advantages are obvious not only for the complete perspective of the functional consequences of ectogenic stimuli but also for the noninvasive, simple and inexpensive nature of the approach.

Liu Wei Di Huang Wan (LW), a well-known formula for invigorating yin-particular kidney yin, was first recorded in “Xiao er Yao Zheng Zhi Jue”, consisting of Radix Rehmanniae Preparata, Fructus Macrocarpii, Rhizoma Dioscoreae Oppositae, Poria, Rhizoma Alismatis and Cortex Moutan Radicis with dose proportion

\* Corresponding author. Tel.: +86 451 8211 0818; fax: +86 451 8213 8380.  
E-mail addresses: [phar\\_research@hotmail.com](mailto:phar_research@hotmail.com), [wxxj@hljucm.net](mailto:wxxj@hljucm.net) (X. Wang).

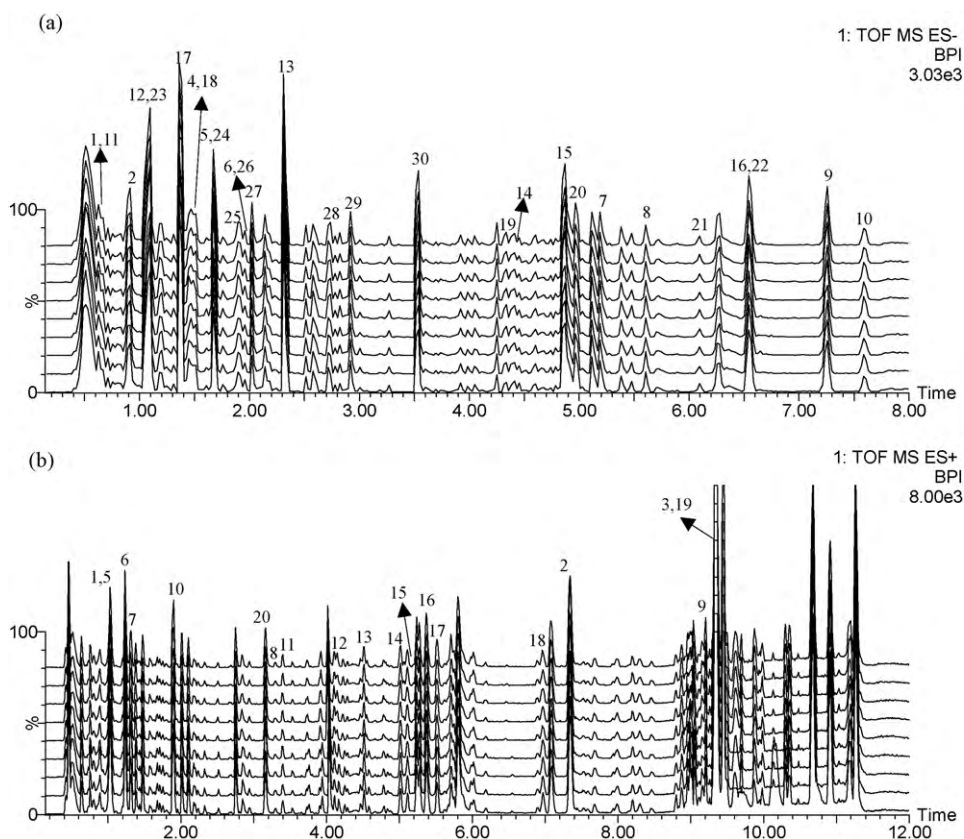


**Fig. 1.** Comparison of fingerprint profiles of nine batches of LW samples by UPLC-HDMS. (a) Negative ESI mode. Peaks 1–10 originated from *Radix Rehmanniae preparata*, peaks 11–13 originated from *Fructus Macrocarpii*, peaks 14–16 originated from *Poria*, peaks 17–22 originated from *Rhizoma Alismatis* and peaks 23–30 originated from *Cortex Moutan Radicis*. (b) Positive ESI mode. Peaks 1–3 originated from *Radix Rehmanniae preparata*, peaks 4–7 originated from *Fructus Macrocarpii*, peaks 8–9 originated from *Poria*, peaks 10–19 originated from *Rhizoma Alismatis* and peak 20 originated from *Cortex Moutan Radicis*.

of 8:4:4:3:3:3. The first three crude drugs are known as “Sanbu” (SB), which invigorate yin of the kidney, liver and spleen, and the rest as “Sanxie” (SX), which attenuate the effects of invigoration. There are usually four kinds of drugs in a Chinese formula, that is the principle drug, the ministerial drug, the adjunctive drug and the messenger drug, they coordinate with each other and enhance the effect of the formula. *Radix Rehmanniae Preparata*, as the principle drug in the famous formula LW, invigorates kidney yin greatly. Both *Fructus Macrocarpii* and *Rhizoma Dioscoreae Oppositae* serve as the ministerial drugs. *Fructus Macrocarpii* invigorates yin of kidney and liver to assist *Radix Rehmanniae Preparata* in invigorating kidney yin. Moreover, liver stores blood and kidney stores essence, essence and blood sharing the same origin, so invigorating liver yin could also assist in invigorating kidney yin. *Rhizoma Dioscoreae Oppositae* invigorates yin of kidney and spleen to assist in invigorating kidney yin. The kidney is the origin of congenital constitution and the spleen is the source of generating Qi and blood. Therefore, invigorating spleen yin could also assist *Radix Rehmanniae Preparata* in invigorating kidney yin. The three drugs mentioned above could invigorate yin of three organs, which are usually called “Sanbu” (three invigoration) in China. The kidney controls water metabolism and kidney yin deficiency leads to deficiency–fire stirring up and malfunction in controlling water, so drugs with the effects of eliminating dampness and nourishing yin for lowering fire should be applied. *Poria*, *Rhizoma Alismatis* and *Cortex Moutan Radicis* serve as the adjunctive drugs in the formula. *Poria* could fortify the spleen and drain dampness, which could also assist *Rhizoma Dioscoreae Oppositae* in invigorating the spleen. *Rhizoma Alismatis* eliminates dampness and turbid to attenuate the excessive invigoration effect of *Radix Rehmanniae Preparata*. *Cortex Moutan Radicis*

clears deficient heat to prevent ministerial fire from damaging yin. These three drugs could eliminate dampness and clear deficient heat and ministerial fire, which are usually called “SanXie” (three eliminate) in China. In a word, “SanBu” coordinates with “SanXie” to replenish kidney essence and LW is applied to treat kidney yin deficiency in clinic. Kidney yin deficiency is a common disease in China, especially for old people. However, with the increasing pace of life, many young people begin to suffer from this disease. Therefore, the present study was undertaken to investigate the metabolic profiling of rats with kidney yin deficiency induced by thyroxine and reserpine as well as the therapeutic effects of LW, SB and SX to mine the differentiating metabolites of this disease for clinic diagnosis and to explore the therapeutic mechanism of LW on both the biochemical and metabonomic levels.

## 2. Experimental

### 2.1. Chemicals and reagents

The six crude drugs, *Radix Rehmanniae preparata*, *Rhizoma Dioscoreae Oppositae*, *Fructus Macrocarpii*, *poria*, *Rhizoma Alismatis* and *Cortex Moutan Radicis*, were purchased from the Harbin Tongrentang Drugstore and were authenticated by Professor Xijun Wang of the Department of Pharmacognosy, Heilongjiang University of Chinese Medicine. The crude drugs were made into honeyed pills (LW, SB, SX) according to the instructions recorded in *Pharmacopoeia of the People's Republic of China* (2005 edition) on page 401–402. The three kinds of pills were then cut into pieces, immersed 10 times in methanol for an hour each time and ultrasonically extracted three times for 40 min each. Finally the filtrate

was combined, and solvents were recycled. The extracts of LW, SB and SX pills were dissolved in distilled water with concentrations of crude drugs at 1.2 g/ml, 0.768 g/ml and 0.432 g/ml, respectively, and stored at 4 °C for animal experimental usage. The UPLC chart of LW extracts is shown in Fig. 1. Altogether, 50 compounds (30 in the negative mode, 20 in the positive mode) have been detected in LW, and these will be reported in another paper (unpublished).

Acetonitrile (HPLC grade) was purchased from Sigma–Aldrich (MO, UK); formic acid (analytical grade) was purchased from the Beijing Reagent Company (Beijing, China); the deionized water was purified by a Milli-Q system (Millipore, Bedford, MA, USA); thyroxine tablets were purchased from Shanghai Industrial United Holdings Great Wall Pharmaceutical Co. Ltd. (Shanghai, China); reserpine injections were purchased from Guangdong Bangmin Pharmaceutical Co. Ltd. (Guangdong, China). The powder of the thyroxine tablets and reserpine injection were dissolved in distilled water with concentrations at 16 mg/ml and 0.1 mg/ml, respectively. Pentobarbital sodium was purchased from the Shanghai Chemical Agent Company of China Medicine Clique (Shanghai, China); the assay kits for estradiol (E2), testosterone (T), thyroxine (T4), triiodothyronin (T3) and cortisol (Cort) were purchased from the Beijing North Biotechnology Institute (Beijing, China); the assay kits for cAMP and cGMP were purchased from the Shanghai University of Chinese Medicine (Shanghai, China); the assay kits for immunoglobulin M (IgM) and immunoglobulin G (IgG) were purchased from the Shanghai Sailor Biotechnology Limited Company (Shanghai, China).

## 2.2. Animal handling and sampling

Sixty male Wistar-derived rats (age, 6 weeks; bodyweight, 200 ± 20 g), provided by the GLP Centre of the Heilongjiang University of Chinese Medicine, were randomly divided into 6 groups with 10 rats in each: the control, model I, model II, LW, SB and SX groups. All animals were kept in the standard environment in the GLP Centre and allowed to acclimatize in metabolism cages for 1 week prior to treatment. Pre-dose urine was collected as the self-blank. The rats in the control group were administered with distilled water in the whole procedure for 20 consecutive days and anaesthetized by intraperitoneal injection of 1% pentobarbital sodium (0.15 ml/100 g body weight) on day 21. Blood was collected from the hepatic portal vein and then was centrifuged at 3500 rpm for 15 min at 4 °C. The supernatants were immediately frozen, stored at –20 °C and thawed before analysis. The serum was used for biochemical indicator detection according to the instructions of commercial kits. The rats in the model I group were administered with thyroxine and reserpine for 10 consecutive days and on day 11 the rats were sacrificed as that in control group. The rats in the model II group were administered with thyroxine and reserpine for 10 consecutive days, then administered with distilled water for another 10 days, and on day 21 the rats were sacrificed as that in control group. The rats in the LW, SB and SX groups were administered with thyroxine and reserpine for 10 consecutive days, then administered with extracts of LW (12 g crude drug/kg body weight), SB (7.68 g crude drug/kg body weight) and SX (4.32 g crude drug/kg body weight) respectively for another 10 days, and on day 21 the rats were sacrificed as that in control group. The whole procedure of administration for each group was shown in Table 1. Urine was collected daily (8:00 am) from metabolism cages at ambient temperature throughout the whole procedure and centrifuged at 13,000 rpm at 5 °C for 15 min, and the supernatants were stored frozen at –20 °C until analysis. Although not all the urine would be analyzed using UPLC-HDMS, the urine would be collected every day in order to making all the rats be in the same condition. The changes in environment will lead to changes in metabolic profiling.

**Table 1**

The whole procedure of administration for each group.

Groups	Days	
	1–10 days	11–20 days
Control group	H <sub>2</sub> O	H <sub>2</sub> O
Model I group	Thyroxine and reserpine	–
Model II group	Thyroxine and reserpine	H <sub>2</sub> O
LW group	Thyroxine and reserpine	LW
SB group	Thyroxine and reserpine	SB
SX group	Thyroxine and reserpine	SX

After all the urine samples were collected, a “quality control” (QC) sample was made. 10 urine samples were randomly selected from the last day urine of each group, and 1 ml urine was taken from each one, then the 10 ml urine was mixed together as the QC sample. The QC sample was used for the optimization of UPLC-MS conditions, as it contained most of the information of the urine samples. Every day, after the instrument was calibrated, the QC sample was firstly analyzed to test the stability of the instrument, making sure the instrument was in the same condition during the whole analytical procedure.

The collected samples of rat serum of each group were characterized on a Beckman-Counter Access 2 Immune analyzer by following clinical chemical parameters according to the corresponding method: T3, T4, Cort, T, E2, cAMP and cGMP. IgM and IgG were analyzed on an Automated Synchron LX20 Beckman Coulter analyzer according to the instructions of the assay kits. The biochemical analysis was done in the affiliated hospital of our university.

## 2.3. UPLC-Q-TOF-HDMS

Urine samples were centrifuged again at 13,000 rpm at 5 °C for 15 min, the supernatants were diluted 10 times with deionized water and 4- $\mu$ l aliquots were transferred to autosampler vials for analysis. The autosampler was maintained at a temperature of 4 °C for the duration of the analysis. The UPLC-MS analysis was performed on a Waters ACQUITY UPLC system (Waters Corporation, Milford, USA) coupled with a Waters Micromass Q-tof microTM Synapt High Definition Mass Spectrometer (Manchester, UK) equipped with electrospray ionization. The data were recorded by MassLynx V4.1 (Waters Corporation, Milford, USA), the MarkerLynx Application Manager (Waters Corporation, Milford, USA) was used for the peak detection and the EZinfo software was used for the PCA, PLS-DA and OPLS analyses. The EZinfo software was included in the MarkerLynx Application Manager and can be applied directly.

For the reversed-phase UPLC analysis, the ACQUITY UPLCTM BEH C18 column (100 mm × 2.1 mm i.d., 1.7  $\mu$ m, Waters Corporation, Milford, USA) was used. The column was eluted with a linear gradient of 1–20% B over 1.0–6.0 min, 20–35% B over 6.0–8.5 min, 35–43% B over 8.5–9.0 min and 43–100% B over 9.0–9.5 min. The composition was held at 100% B for 1.0 min, returned to 1% B for 11.0 min and then held for 2 min at an eluent flow rate of 500  $\mu$ l/min, where mobile phase A consisted of 0.1% formic acid in deionized water and mobile phase B consisted of 0.1% formic acid in acetonitrile.

For the UPLC-HDMS analysis, the optimal conditions were as follows: the source temperature was set at 110 °C with a cone gas flow of 50 l/h, a desolvation gas temperature of 300 °C and a desolvation gas flow of 500 l/h. In negative ion mode, the capillary voltage was set at 2.4 V, the sample cone voltage was set 30 V and the extraction cone voltage was set 4.0 V. In positive ion mode, the capillary voltage was set at 2.6 V, the sample cone voltage was set 30 V and the extraction cone voltage was set 3.0 V. A scan time of 0.3 s with an inter-scan delay of 0.1 s was used through-

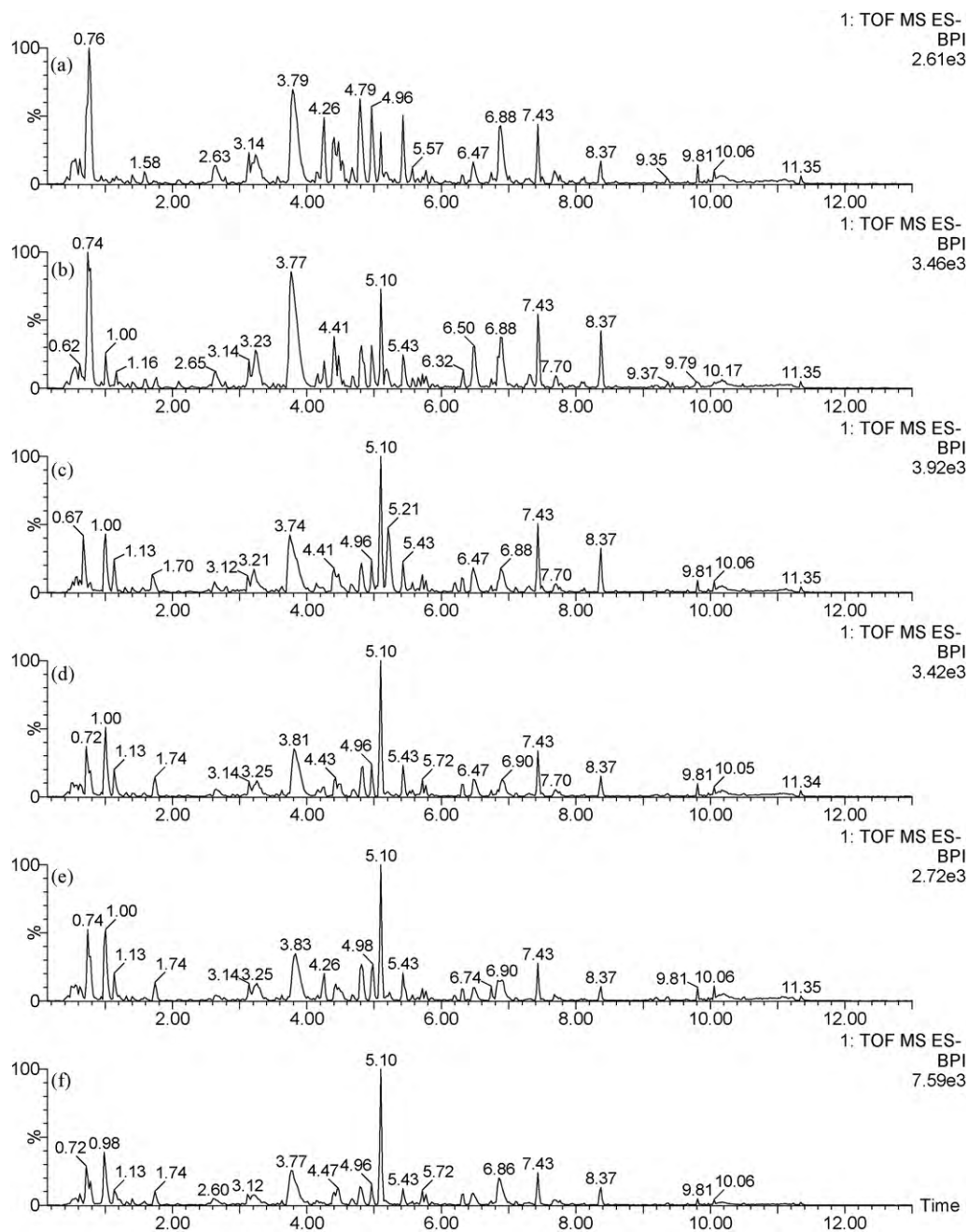


**Fig. 2.** BPI chromatograms of (a) control rats, (b) model I rats, (c) LW-treated rats, (d) SB-treated rats and (e) SX-treated rats. (f) Model II rats urine samples on the last day analyzed by UPLC-HDMS in negative ESI mode.

**Table 2**

Blood biochemical examinations in different groups, mean  $\pm$  SD,  $n = 10$ .

	T3 (ng/ml)	T4 (ng/ml)	Cort (ng/ml)	T (ng/ml)	E2 (pg/ml)	cAMP (pM/ml)	cGMP (pM/ml)	IgM (g/l)	IgG (g/l)
Con.	0.87 $\pm$ 0.20	99.74 $\pm$ 16.93	303.15 $\pm$ 58.35	4.61 $\pm$ 2.06	64.84 $\pm$ 18.77	0.23 $\pm$ 0.03	0.032 $\pm$ 0.007	1.28 $\pm$ 0.63	8.47 $\pm$ 2.34
Mod I	0.90 $\pm$ 0.51	119.54 $\pm$ 27.20*	383.57 $\pm$ 48.03**	2.66 $\pm$ 0.93*	82.22 $\pm$ 20.16*	0.24 $\pm$ 0.02	0.034 $\pm$ 0.009	0.70 $\pm$ 0.22	4.78 $\pm$ 1.30**
Mod II	0.89 $\pm$ 0.40	117.75 $\pm$ 17.84*	323.96 $\pm$ 59.65	2.93 $\pm$ 1.61*	81.08 $\pm$ 14.96*	0.23 $\pm$ 0.03	0.034 $\pm$ 0.007	1.01 $\pm$ 0.71	5.19 $\pm$ 1.36**
LW	0.86 $\pm$ 0.16	99.97 $\pm$ 14.83#	306.17 $\pm$ 55.14#	5.02 $\pm$ 2.19#	65.43 $\pm$ 12.56#	0.23 $\pm$ 0.03	0.033 $\pm$ 0.007	1.41 $\pm$ 0.96	7.68 $\pm$ 1.18##
SB	0.81 $\pm$ 0.17	107.46 $\pm$ 21.84	345.87 $\pm$ 47.40	4.67 $\pm$ 1.80#	72.10 $\pm$ 14.08	0.22 $\pm$ 0.03	0.040 $\pm$ 0.009	1.12 $\pm$ 0.53	7.19 $\pm$ 1.64##
SX	0.92 $\pm$ 0.37	102.14 $\pm$ 23.47	316.27 $\pm$ 60.70	4.16 $\pm$ 1.37	77.06 $\pm$ 13.29	0.25 $\pm$ 0.03	0.040 $\pm$ 0.004	0.97 $\pm$ 0.34	5.59 $\pm$ 1.93

\* Significant difference from control at  $p < 0.05$ .

\*\* Significant difference from control at  $p < 0.001$ .

# Significant difference from model I at  $p < 0.05$ .

## Significant difference from model I at  $p < 0.001$ .

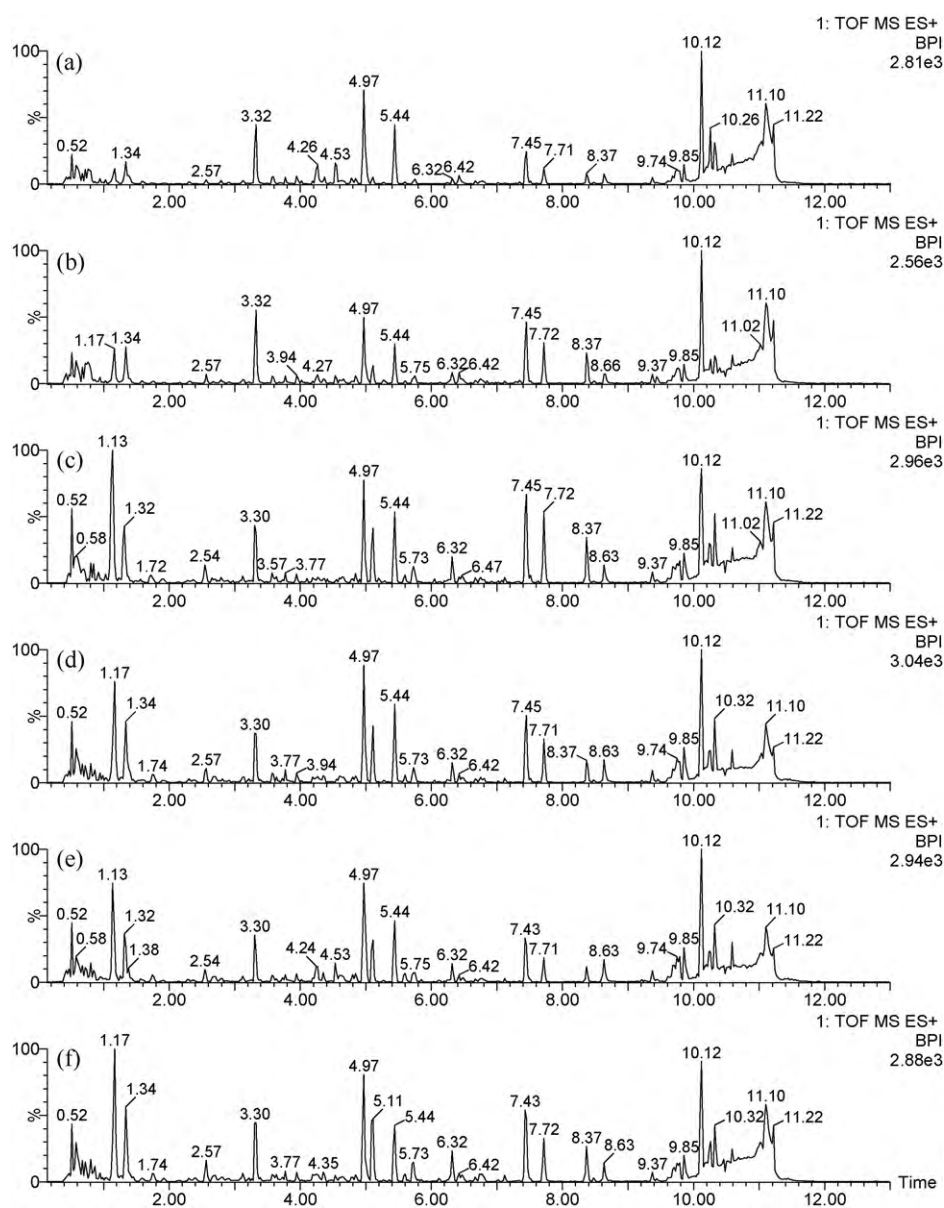


**Fig. 3.** BPI chromatograms of (a) control rats, (b) model I rats, (c) LW-treated rats, (d) SB-treated rats and (e) SX-treated rats. (f) Model II urine samples on the last day analyzed by UPLC–HDMS in positive ESI mode.

out, with Trap CE at 6.0V and Transfer CE at 4.0V. A lock-mass of leucine enkephalin at a concentration of 200 pg/ml in acetonitrile (0.1% formic acid): H<sub>2</sub>O (0.1% formic acid) (50:50, v/v) for the positive ion mode ( $[M+H]^+ = 556.2771$ ) and negative ion mode ( $[M-H]^- = 554.2615$ ) were employed via a lock spray interface. Data were collected in centroid mode, the lock spray frequency was set at 5 s and the lock mass data were averaged over 10 scans for correction. A “purge–wash–purge” cycle was employed on the autosampler with 90% aqueous formic acid used for the wash solvent and 0.1% aqueous formic acid used as the purge solvent. This process ensured that the carry-over between injections was minimized. The mass spectrometric data were collected in full scan auto mode from 0 to 13 min in both positive and negative ion mode.

#### 2.4. Data analysis

The UPLC–HDMS data were analyzed using the Micromass MarkerLynx Applications Manager. MarkerLynx incorporates a peak deconvolution package, which allows detection and reten-

tion time alignment of the peaks eluting in each chromatogram. The processed data were then analyzed with EZinfo software. The biochemical data were analyzed using SPSS 16.0.

### 3. Results

#### 3.1. Biochemical analysis

The sera marker (namely T4, Cort and E2) of the model I group were increased compared with those of the control group, and levels of T and IgG were decreased significantly compared with those of the control group after thyroxine and reserpine treatment. These biochemical indicators of the model II group, namely T4 and E2, were increased significantly compared with those of the control group, and levels of T and IgG were decreased significantly compared with those of the control group. These results indicated that the rodent model of kidney yin deficiency was successfully reproduced, and the rats had not recovered 10 days after administration of thyroxine and reserpine was stopped, which is consistent with

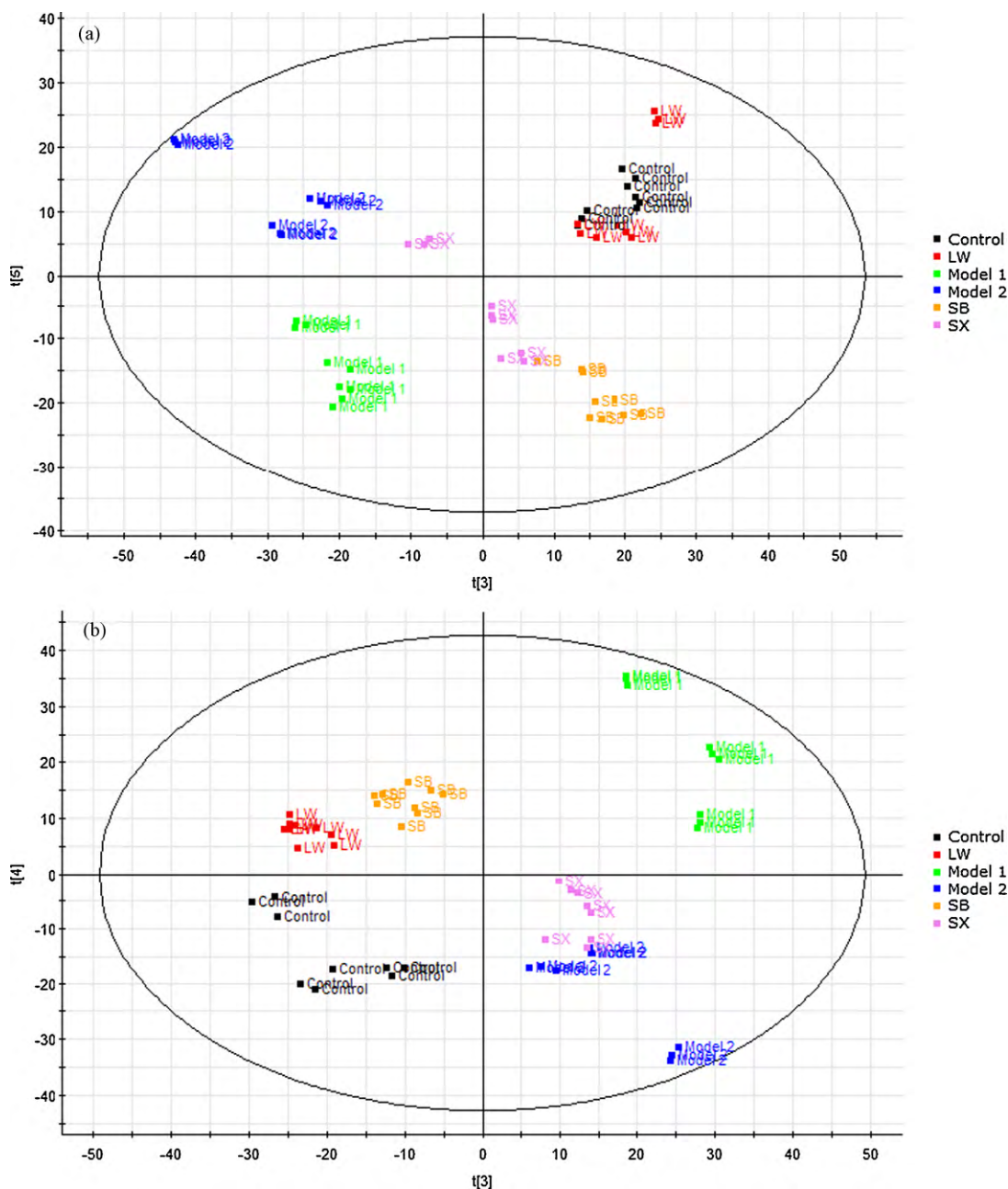


Fig. 4. PCA score plots of urine samples collected from different treatment groups of rats (a) in negative ESI mode and (b) in positive ESI mode.

the clinical report that the potency of the two medicines lasted for several weeks after cessation. These biochemical indicators, namely T4, Cort, T, E2 and IgG, were significantly regulated back towards their baseline levels as a result of LW administration, demonstrating that LW might have some therapeutic effect on the rat model. However, SB and SX, components of LW, did not show significantly therapeutic effects in this rat model (only T and IgG were changed significantly in the SB group), indicating that the combination of the six drugs was reasonable (Table 2).

### 3.2. Metabolic profiling analysis

Using the optimal UPLC-HDMS conditions described in Section 2.3, the representative Based Peak Intensity (BPI) chromatograms for the reversed-phase UPLC-HDMS analysis of urine samples collected from representative rats for each of the different groups are

presented in Figs. 2 and 3. Urine samples on the last day from each group were used for UPLC-HDMS analysis, that was for model I group, it was on day 11, for the others, on day 21. Some differences could be visually noted among these chromatograms. Low molecular mass metabolites could be separated well in the short time of 13 min due to the minor particles (sub-1.7  $\mu\text{m}$ ) of UPLC.

### 3.3. PCA analysis

In order to clearly differentiate among groups, unsupervised pattern recognition PCA, a chemometric model that reduces a matrix of data to its lowest dimension of the most significant factors, was used for analyzing the chromatographic data. Before the urinary data was subjected to PCA model using EZinfo software, the ions that were not contained in the urine sample of the control group were excluded. Therefore, the separations could not be

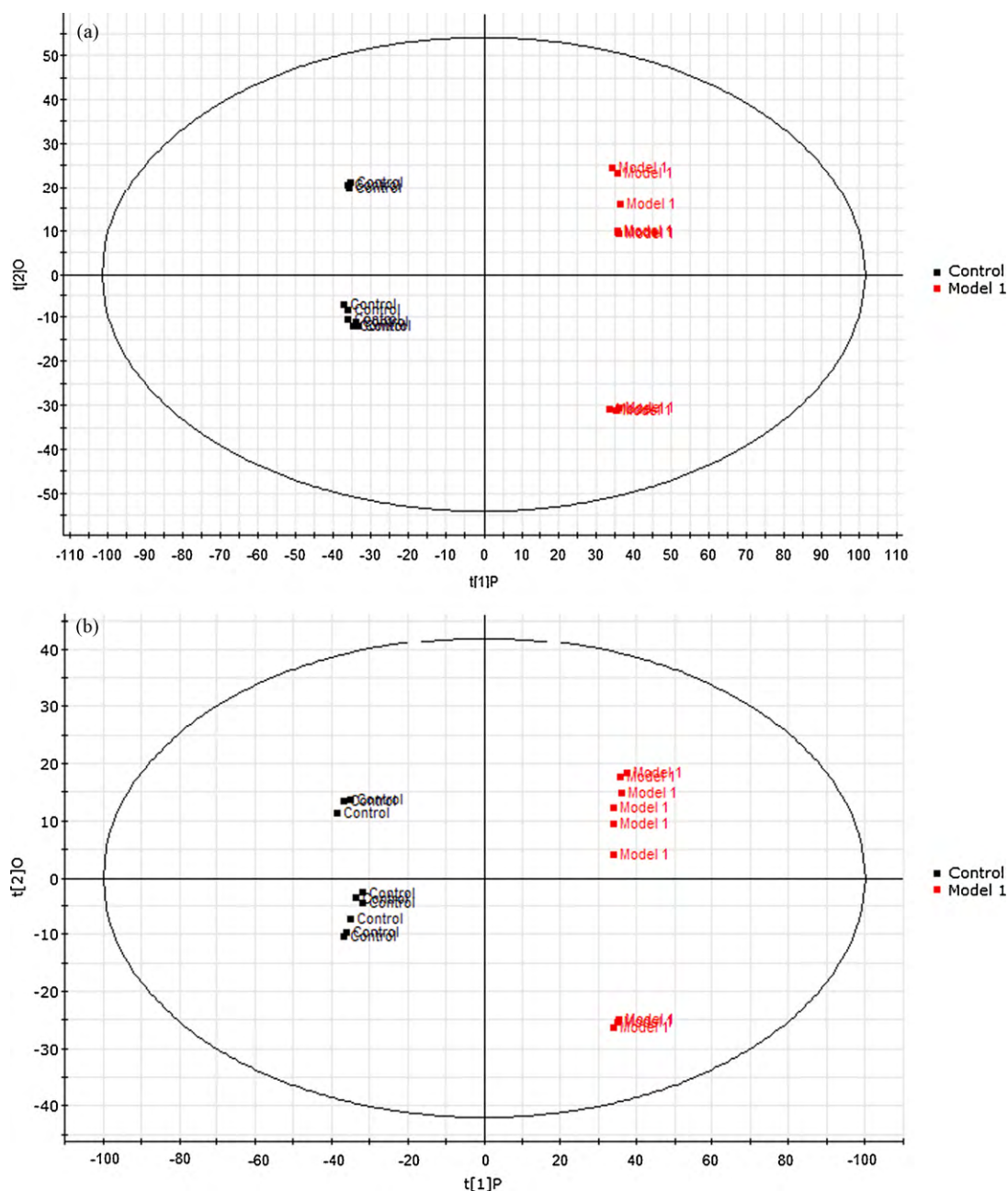


Fig. 5. OPLS score plot of the control and model I groups in (a) negative ESI mode and (b) positive ESI mode.

derived by the metabolites of 3 agents (LW, SB, SX). PCA score plots separated urine samples into different blocks, and samples subjected to the same treatment were located on the same trajectory, indicating that treatments have greatly disturbed the normal urine metabolic profiles of rats (Fig. 4). Urine from the model I group on day 11 was the furthest from control group, suggesting the metabolic profiles have significantly changed as a result of thyroxine and reserpine administration. Rats in model II group were administrated with thyroxine and reserpine for 10 consecutive days, then administrated with water for another 10 days and urine on day 21 was analyzed as the samples of model II group. The perturbation of metabolic profiles of the model II group shifted slightly towards baseline, however, it was still separated from the control group, demonstrating that the perturbation was not com-

pletely eliminated after stimulus from thyroxine and reserpine was removed, which was consistent with a clinical report that the potency of the two medicines lasts for several weeks after administration. Urine of the SX-treated group on day 21 was located near the model I group, indicating they could have similar metabolic profiles. Urines of the LW and SB-treated groups on day 21 were located near the control group, especially the LW-treated group. Some of the samples in the control and LW groups clustered, suggesting that the LW and control groups could have similar metabolic profiles, and that LW could assist recovery of the animals from earlier thyroxine and reserpine treatment. The PCA analysis of the chromatographic data identified the control and the treated rats based on the differences in their metabolic profiles, demonstrating that a rodent model of kidney yin deficiency was successfully reproduced,

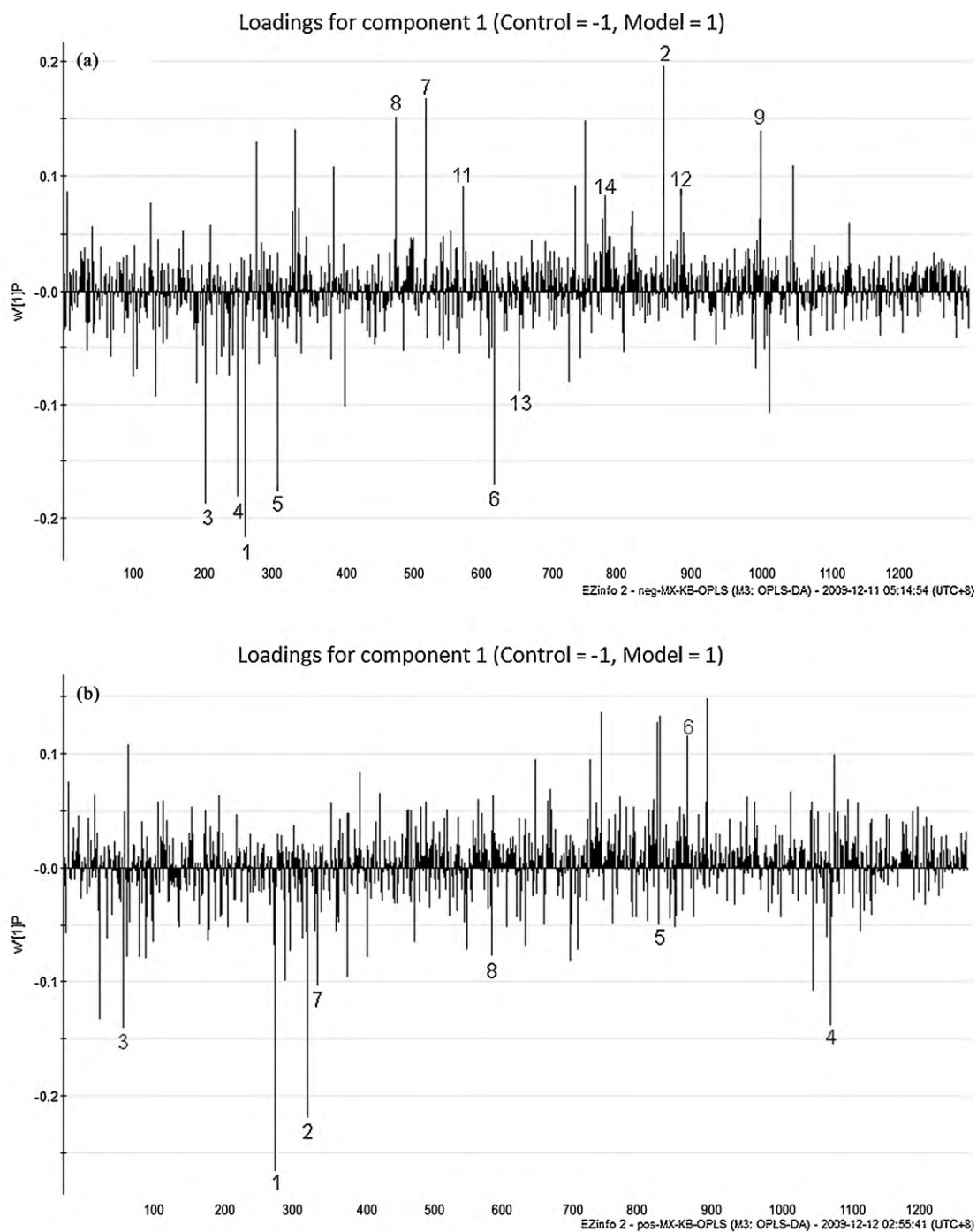


Fig. 6. Loadings for component 1 in (a) negative ESI mode and (b) positive ESI mode.

and the classic formula of LW showed significant therapeutic effects on the rodent model, which was consistent with blood biochemistry examinations. SB and SX as part of the classic formula did not show noticeable therapeutic effects on the rodent model, properly indicating that indicating that the combination of the six drugs was reasonable.

#### 3.4. OPLS-DA analysis

In order to obtain better discrimination between the control and model I groups, the OPLS-DA approach was applied to the metabolic profiles. OPLS-DA score plots separated urine samples

into two blocks, especially in the component P1 direction, and component P2 properly explained individual variation in each group (Fig. 5). Loadings for component P1 indicated the content of each ion in the control and model I groups; the Y+ axis represented the model I group; the Y- axis represented the control group; the X-axis represented the number of detected ions (Fig. 6). Arabic numbers mark the differentiating metabolites for the rodent model of kidney yin deficiency and were compatible with the serial numbers in Tables 3 and 4, which are detailed in the following section. To exhibit the responsibility of each ion for these variations more intuitively, S-plots and VIP-value plots were combined (Fig. 7). The black point graph is the S-plot, and most of the ions were clus-



**Table 3**  
Potential biomarkers identified in negative ESI mode.

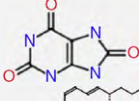
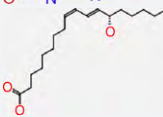
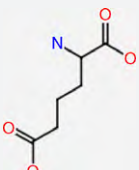
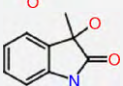
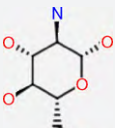
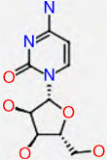
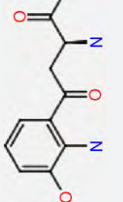
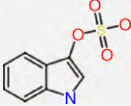
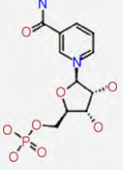
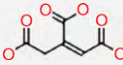
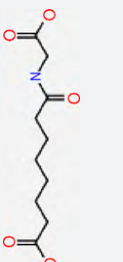
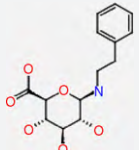
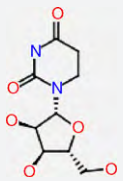
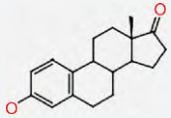
NO	VIP values	Rt.M <sup>-</sup>	Actual.M	Proposed compound	Content variance	[M-H] <sup>-</sup>	MS/MS	Losses	Proposed structure
1.	7.84	0.71.167.0196	168.0283	Uric acid C <sub>5</sub> H <sub>4</sub> N <sub>4</sub> O <sub>3</sub>	↑	167	111 87 85	-C <sub>2</sub> H <sub>2</sub> NO -C <sub>3</sub> N <sub>2</sub> O -C <sub>3</sub> NO <sub>2</sub>	
2.	7.06	5.15.295.2202	296.2351	13S-hydroxyoctadecadienoic acid 13-HODE C <sub>18</sub> H <sub>32</sub> O <sub>3</sub>	↓	295	253  124	-C <sub>3</sub> H <sub>6</sub>  -C <sub>10</sub> H <sub>19</sub> O <sub>2</sub>	
3.	6.80	4.97.160.0582	161.0688	Amino adipic acid C <sub>6</sub> H <sub>11</sub> NO <sub>4</sub>	↑	160	142 131 104	-H <sub>2</sub> O -NO -C <sub>2</sub> O <sub>2</sub>	
4.	6.39	5.46.162.0548	163.0633	3-Methylendioxyindole C <sub>9</sub> H <sub>9</sub> NO <sub>2</sub>	↑	162	147  144 134 132 120	-CH <sub>3</sub>  -H <sub>2</sub> O -CO -CH <sub>2</sub> O -CNO	
5.	6.19	4.26.178.0712	179.0794	Glucosamine C <sub>6</sub> H <sub>13</sub> NO <sub>5</sub>	↑	178	134  77	-CH <sub>2</sub> NO  -C <sub>4</sub> H <sub>5</sub> O <sub>3</sub>	
6.	6.19	4.77.242.0421	243.0855	Cytidine C <sub>9</sub> H <sub>13</sub> N <sub>3</sub> O <sub>5</sub>	↑	242	162 134 119	-C <sub>3</sub> N <sub>2</sub> O -C <sub>4</sub> H <sub>2</sub> N <sub>3</sub> O -C <sub>5</sub> H <sub>3</sub> N <sub>2</sub> O <sub>2</sub>	
7.	6.03	1.05.223.9823	224.0797	L-3-Hydroxykynurenine C <sub>10</sub> H <sub>12</sub> N <sub>2</sub> O <sub>4</sub>	↓	223	179  143 115 97 81	-CO <sub>2</sub>  -COOH-H <sub>2</sub> O -NH <sub>3</sub> -C <sub>6</sub> H <sub>6</sub> NO -C <sub>6</sub> H <sub>10</sub> N <sub>2</sub> O -C <sub>6</sub> H <sub>10</sub> N <sub>2</sub> O <sub>2</sub>	
8.	5.48	3.72.212.0012	213.0096	Indoxyl sulfate C <sub>8</sub> H <sub>7</sub> NO <sub>4</sub> S	↓	212	132  104	-O <sub>3</sub> S  -O-S-CH <sub>2</sub> N	
9.	5.01	6.39.333.0426	334.0566	Nicotinamide ribotide C <sub>11</sub> H <sub>15</sub> N <sub>2</sub> O <sub>8</sub> P	↓	333	253  223 209 160 135	-HO <sub>3</sub> P  -HNO <sub>4</sub> P -CHO <sub>5</sub> P -C <sub>2</sub> H <sub>8</sub> NO <sub>6</sub> P -C <sub>4</sub> H <sub>9</sub> NO <sub>6</sub> P	
10.	4.67	3.13.173.0088	174.0164	cis-Aconitic acid C <sub>6</sub> H <sub>6</sub> O <sub>6</sub>	↓	173	93	-CH <sub>4</sub> O <sub>4</sub>	
11.	3.26	1.73.230.1134	231.1107	Suberylglycine C <sub>10</sub> H <sub>17</sub> NO <sub>5</sub>	↓	230	213  187 145	-OH  -CO <sub>2</sub> -C <sub>3</sub> HO <sub>3</sub>	

Table 3 (Continued)

NO	VIP values	Rt.M <sup>-</sup>	Actual.M	Proposed compound	Content variance	[M-H] <sup>-</sup>	MS/MS	Losses	Proposed structure
12.	3.20	5.11.296.1378	297.1212	Phenethylamine glucuronide C <sub>14</sub> H <sub>19</sub> NO <sub>6</sub>	↓	296	253 124 94	-CO <sub>2</sub> -C <sub>8</sub> H <sub>12</sub> O <sub>4</sub> -C <sub>9</sub> H <sub>16</sub> NO <sub>4</sub>	
13.	3.17	4.48.245.0795	246.0852	5,6-Dihydrouridine C <sub>9</sub> H <sub>14</sub> N <sub>2</sub> O <sub>6</sub>	↑	245	165 121 119	-2OH-CH <sub>2</sub> O <sub>2</sub> -C <sub>6</sub> H <sub>4</sub> O <sub>3</sub> -C <sub>5</sub> H <sub>4</sub> NO <sub>3</sub>	
14.	3.01	1.15.269.1514	270.1620	Estrone C <sub>18</sub> H <sub>22</sub> O <sub>2</sub>	↓	269	227 209 183 112	-H <sub>2</sub> O -C <sub>2</sub> H <sub>4</sub> O <sub>2</sub> -C <sub>5</sub> H <sub>10</sub> O -C <sub>11</sub> H <sub>9</sub> O	

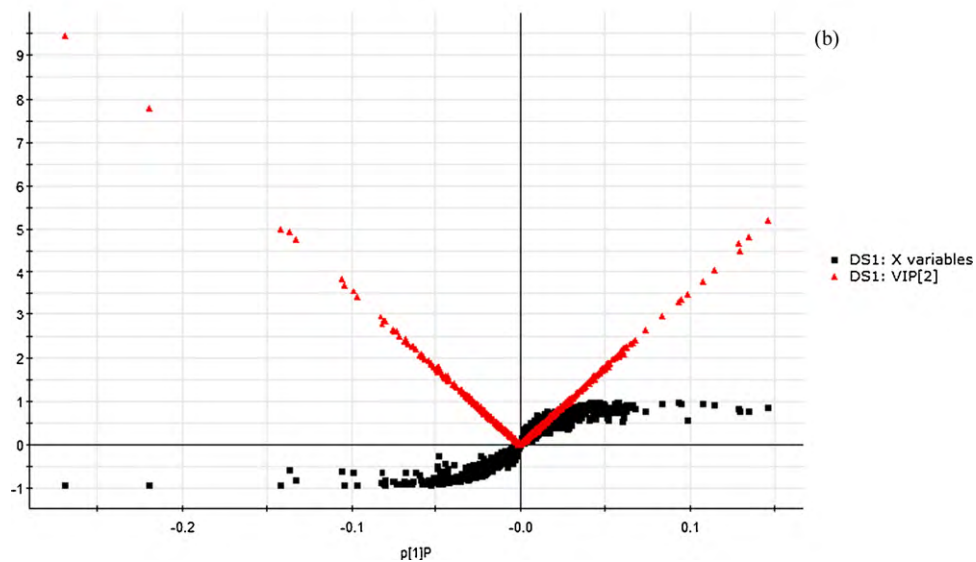
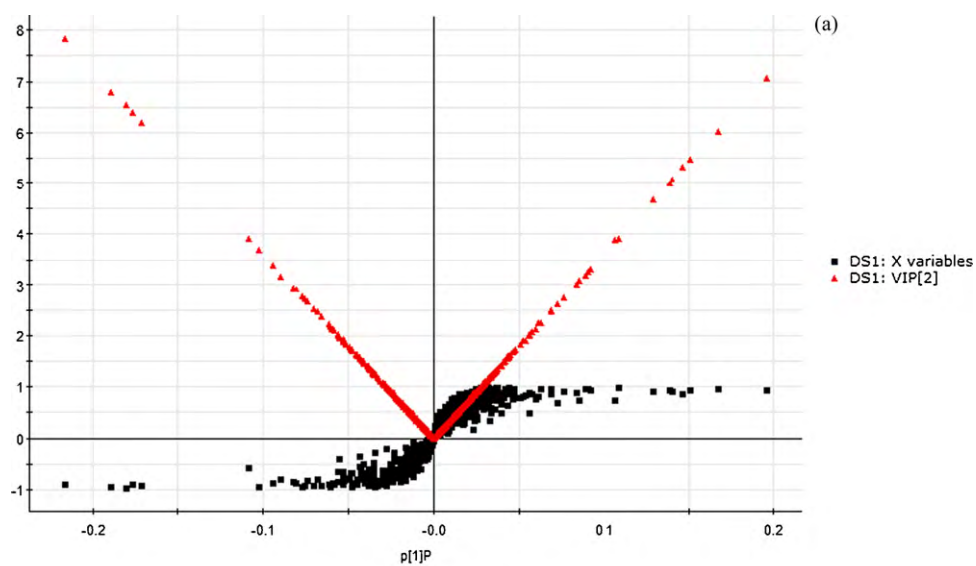
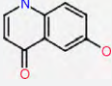
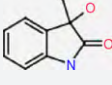
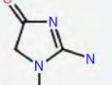
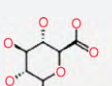
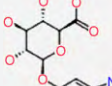
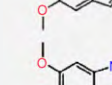
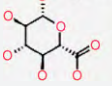
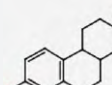
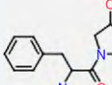
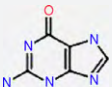
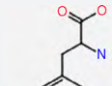
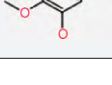


Fig. 7. Combination of S-plot and VIP values in (a) negative ESI mode and (b) positive ESI mode.

**Table 4**  
Potential biomarkers identified in positive ESI mode.

NO	VIP values	Rt.M*	Actual_M	Proposed compound	Content variance	[M+H] <sup>+</sup>	MS/MS	Losses	Proposed structure
1.	9.46	4.96.162.0502	161.0477	4,6-Dihydroxyquinoline C <sub>9</sub> H <sub>7</sub> NO <sub>2</sub>	↑	162	144 116	-H <sub>2</sub> O -CH <sub>4</sub> NO	
2.	7.79	5.47.164.659	163.0633	3-Methyldioxyindole C <sub>9</sub> H <sub>9</sub> NO <sub>2</sub>	↑	164	146 122 119	-H <sub>2</sub> O -CNO -CH <sub>3</sub> NO	 
3.	5.01	0.62.114.0710	113.0589	Creatinine C <sub>4</sub> H <sub>7</sub> N <sub>3</sub> O	↑	114	113	-H	
4.	4.94	5.00.340.1013	339.0954	6-Hydroxy-5-methoxyindole glucuronide or 5-Hydroxy-6-methoxyindole glucuronide C <sub>15</sub> H <sub>17</sub> NO <sub>8</sub>	↑	340	164 146 122 118	-C <sub>9</sub> H <sub>6</sub> NO <sub>3</sub> -C <sub>9</sub> H <sub>6</sub> NO <sub>4</sub> -C <sub>11</sub> H <sub>8</sub> NO <sub>4</sub> -C <sub>10</sub> H <sub>8</sub> NO <sub>5</sub>	  
5.	4.67	1.15.271.1372	270.1620	Estrone C <sub>18</sub> H <sub>22</sub> O <sub>2</sub>	↓	271	229 166 116	-C <sub>3</sub> H <sub>5</sub> -C <sub>7</sub> H <sub>5</sub> O -C <sub>9</sub> H <sub>15</sub> O <sub>2</sub>	
6.	4.06	5.10.279.1281	278.1267	L-phenylalanyl-L-hydroxyproline C <sub>14</sub> H <sub>18</sub> N <sub>2</sub> O <sub>4</sub>	↓	279	237 192 175 148 120	-C <sub>2</sub> H <sub>2</sub> O -C <sub>3</sub> H <sub>5</sub> NO <sub>2</sub> -C <sub>3</sub> H <sub>4</sub> O <sub>4</sub> -C <sub>4</sub> H <sub>5</sub> NO <sub>4</sub> -C <sub>6</sub> H <sub>9</sub> NO <sub>4</sub>	
7.	3.71	0.83.166.0679	165.0651	3-Methylguanaine C <sub>6</sub> H <sub>7</sub> N <sub>5</sub> O	↑	166	149 124 107	-NH <sub>3</sub> -CH <sub>2</sub> N <sub>2</sub> -CH <sub>5</sub> N <sub>3</sub>	
8.	3.32	0.62.212.0930	211.0845	3-Methoxytyrosine C <sub>10</sub> H <sub>13</sub> NO <sub>4</sub>	↑	212	194 166 153 109	-H <sub>2</sub> O -CH <sub>2</sub> O <sub>2</sub> -C <sub>2</sub> H <sub>3</sub> O <sub>2</sub> -C <sub>3</sub> H <sub>5</sub> NO <sub>3</sub>	 

tered around the origin point; only a few of them scattered in the margin region, and just these few ions contributed to the clustering observed in the score plot and were also the differentiating metabolites. The red point graph is the VIP-value plot, which represents the value of each ion. The farther away from the origin, the higher the VIP value of the ions was. The black points and red points were in one-to-one correspondence in the combination.

### 3.5. Differentiating metabolites identification

All the detected ions were arranged in descending order according to VIP values, and the highest VIP value was 7.84 in the negative mode. Combining the results of the OPLS analysis with the amount variation of ions in each group, 24 ions with VIP values exceeding three were selected in the negative mode. At

the same time, the highest VIP value was 9.46 in the positive mode, and 19 ions with VIP values exceeding three were selected. The UPLC-HDMS segregation analysis platform provided the retention time, precise molecular mass and MS/MS data for the structural identification of biomarkers. The precise molecular mass was determined within measurement errors (<5 ppm) by Q-TOF, and meanwhile, the potential elemental composition, degree of unsaturation and fractional isotope abundance of compounds were obtained. The presumed molecular formula was searched in Chemspider, the Human Metabolome Database and other databases to identify the possible chemical constitutions, and MS/MS data were screened to determine the potential structures of the ions.

According to the protocol detailed above, the structures of 14 differentiating metabolites were preliminary identified in

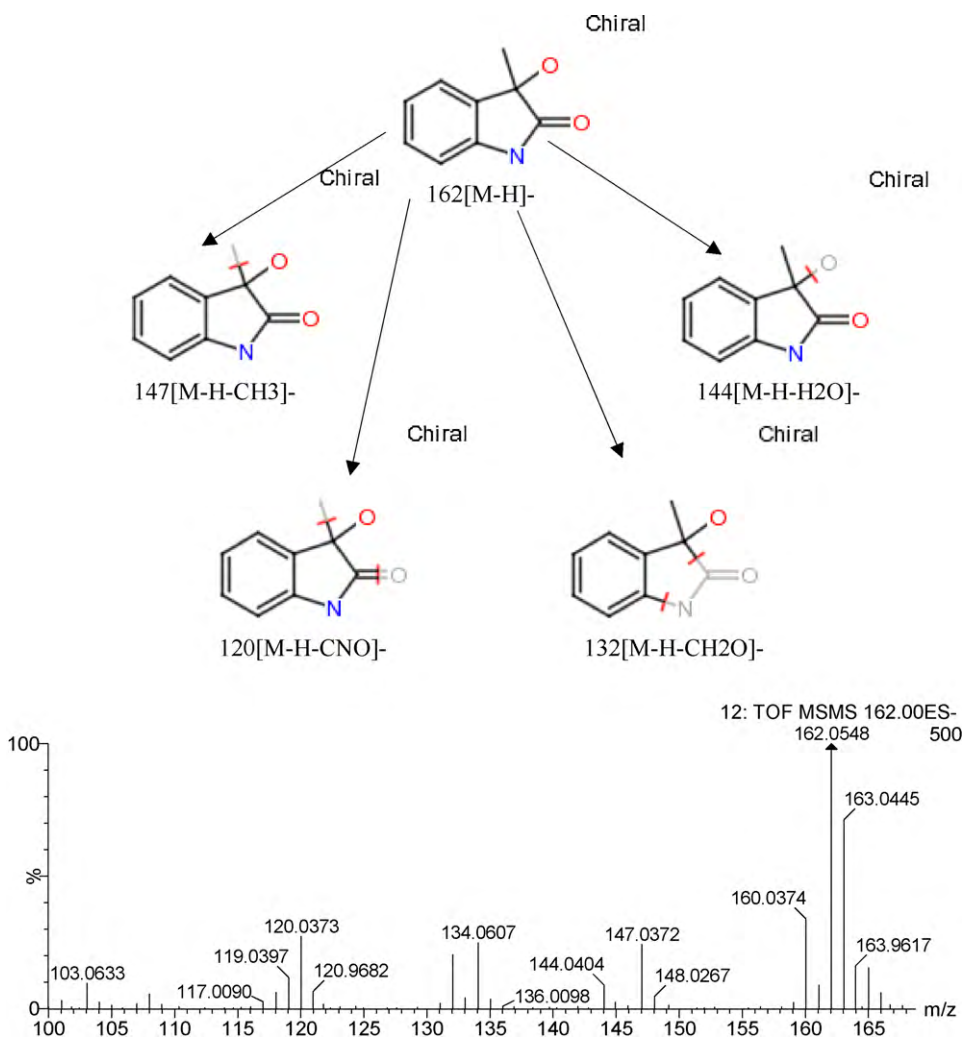


Fig. 8. Chemical structure and mass fragment information of 3-methyldioxyindole in negative ESI mode.

the negative mode and 8 in positive mode (2 in both modes) (Tables 3 and 4). Taking two ions as examples, the identification procedure was as follows. In the negative mode, the ion at  $R_t = 5.46$  and  $[M-H]^- = 162.0548$  has a high VIP value. This ion might contain an odd number of nitrogen atoms because its precise molecular weight was 163.0633, and its molecular formula was speculated as  $C_9H_9NO_2$  from the analysis of its elemental composition and fractional isotope abundance. The degree of unsaturation was calculated as 7, indicating that it was a ring compound. The main fragment ions analyzed by MS/MS screening were  $m/z$  147, 144, 132 and 120, which could be the  $[M-H]^-$  of lost  $-CH_3$ ,  $-H_2O$ ,  $-CH_2O$  and  $-CNO$ , respectively. Finally, it was speculated as 3-methyldioxyindole when researched in databases, and its mass spectrum and structure are displayed in Fig. 8. In the same way, the ion at  $R_t = 4.96$  and  $[M+H]^+ = 162.0502$  has the highest VIP value and it was primarily identified as 4,6-dihydroxyquinoline in the positive mode after searching in the database, and the main fragments were  $m/z$  144 and 116, which could correspond to lost  $-H_2O$  and  $-CH_2N$ , respectively. Its mass spectrum and structure are displayed in Fig. 9. All of the primarily identified potential biomarkers are shown in Tables 3 and 4, and the serial numbers in Tables 3 and 4 are compatible with the Arabic numbers in Fig. 6. The metabolic pathways of biomarkers related to kidney yin deficiency are explained in the discussion.

#### 4. Discussion

The model of kidney yin deficiency is a classic symptom model in Chinese medical science, which was initially studied starting in the 1950s. To date there are eight methods to reproduce this animal model, such as thyroxine, thyroxine with reserpine, hypodesis of the renal artery, febricity herb medicine and others [9–12], among which thyroxine with reserpine is the most common approach, and thus it was employed in the present study. The basic action of thyroxine is to induce synthesis of neonatal protein and regulate the metabolism of protein, fat, carbohydrates, water, salt and vitamins. However, if thyroxine is administered in higher doses, it can lead to dyssynchrony between energy metabolism and physical function, causing iatrogenic hyperthyroidism, whose clinical manifestation is impatience, tremble, hyperhidrosis, heat avoidance, dry mouth, polydipsia, polyphagia, magersucht, palpitation and a powerful-sounding heart beat. Furthermore, it can also immunocompromise animals, causing pathological changes in the immune organs, hypothalamus-pituitary gland-adrenal glands axis, thyroid gland axis and gonad axis functional disorder and dysfunction of the function of autonomic nerves. All of these symptoms are consistent with the clinical manifestation of kidney yin deficiency, and therefore it was feasible to use thyroxine to replicate this disease model. As for reserpine, it could not influence the actions of thyrox-

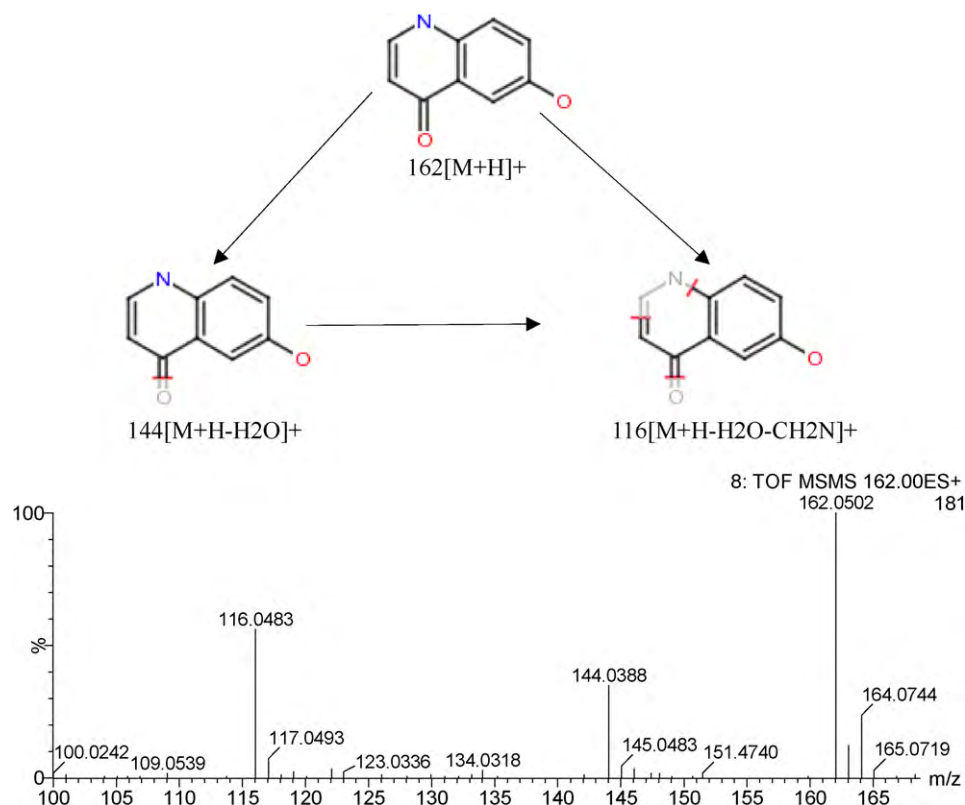


Fig. 9. Chemical structure and mass fragment information of 4,6-dihydroxyquinoline in positive ESI mode.

ine directly but causes hyperfunction of the parasympathetic nerve to assist in reproducing yin deficiency.

Blood biochemistry examinations revealed that marker sera (namely T4, Cort, E2, T and IgG) of the model I group were significantly changed compared with those of the control group, and these biochemical indicators of the model II group were still different from those of the control group after thyroxine and reserpine treatment, indicating that the rodent model of kidney yin deficiency was successfully reproduced, and that the baseline was not restored 10 days after ending the administration of thyroxine and reserpine. These results are consistent with the clinical report that the potency of the two medicines lasted for several weeks after ending the administration. The marker sera (namely T4, Cort, E2, T and IgG) returned to baseline when the model rats were subjected to LW; however, SB and SX as components of LW did not show significant therapeutic effects in this rat model, which properly demonstrated the efficiency of the LW formula.

In order to investigate the pathological essence of kidney yin deficiency induced by thyroxine and reserpine as well as the therapeutic effects of LW, SB and SX, a metabonomic approach based on the UPLC–HDMS technique was employed to demonstrate the urinary metabolic characteristics. Hence, chemometrics such as PCA and OPLS were applied to metabolic data to mine the differentiating metabolites that contributed to the clustering observed in the score plots. Finally, 20 differentiating metabolites were preliminary identified in the negative and positive modes (Tables 3 and 4), which had relationships with the metabolic pathways of tryptophan, lysine, purine, pyrimidine, tricarboxylic acid cycle and others.

In the negative mode, uric acid was the most responsible ion for discrimination; as the terminal metabolite of purines, it is excreted by the kidney and intestinal tract. The content of uric acid increased greatly in the rat model, suggesting that the kidney glomerulus suffered an inflammatory reaction [13], and kidney yin deficiency might have some relationship with

the kidney organ. 13S-hydroxyoctadecadienoic acid (13-HODE) is synthesized in the body from linoleic acid, participates in cell multiplication in several systems and has a close relationship with cell function [14]. The 13-HODE content decreased in the rat model, demonstrating that changes in cell function might affect the metabolism of 13-HODE directly. Lysine plays important roles in the absorption and utilization of protein, nutritional balance, improvement of nervous system function, enhancement of immune system function, prevention of osteoporosis and other systems [15–19]. Normally, the metabolism of lysine is stable and cannot be affected by the dose [16]. In the rat model of kidney yin deficiency, the content of amino adipic acid, a metabolite of lysine, increased significantly, suggesting that the administration of thyroxine and reserpine might have caused dysfunction that changed the metabolism of lysine. 3-Methyldioxyindole is the main metabolite of 3-Methylindole and increased in the rat model, but the relationship between this metabolite and kidney yin deficiency is still uncertain. Glucosamine, a metabolite of aminosaccharide, participates in energy metabolism. Its level greatly increased in the model group, indicating that the energy metabolism of the rat model was disordered, which is consistent with the clinical report of kidney yin deficiency. Cytidine is a nucleoside that is composed of the base cytosine linked to the five-carbon sugar D-ribose. Cytidine is a pyrimidine that, besides being incorporated into nucleic acids, can serve as substrate for the salvage pathway of pyrimidine nucleotide synthesis. Metabolic disorders of pyrimidine suggest that congenital enzyme defects, acquired drugs or foods result in increases in the metabolites of pyrimidine in blood or urine. Cytidine as a metabolite of pyrimidine increased greatly in the urine of the model group, indicating a metabolic disorder of pyrimidine induced by thyroxine and reserpine [20]. L-3-Hydroxykynurenine (L-3-HK) is a metabolite in the kynurenine pathway, the major route of tryptophan degradation in mammals, and indoxyl sulphate is a metabolite in another

tryptophan degradation pathway. Tryptophan is one of the eight essential amino acids in the body, playing a fundamental role in physiology and biochemistry, and can stabilize polyribosomes to regulate humoral immunity [21]. The urine contents of L-3-HK and indoxyl sulphate decreased obviously, suggesting that the rats were immuno-compromised. Nicotinamide ribotide (NMN) is an important intermediate metabolite in the nicotinate and nicotinamide metabolic pathway. Mammals predominantly use nicotinamide rather than nicotinic acid as a precursor for NAD biosynthesis. Instead of the deamidation to nicotinic acid, nicotinamide is directly converted to NMN by nicotinamide phosphoribosyltransferase. NMN is an important metabolite for the maintenance of normal NAD biosynthesis, and circulating NMN levels may play an important role in regulating cell function in physiological and pathophysiological conditions. However, NMN decreased significantly in the urine of the rat model and resulted in changes to the normal cell function and substance metabolism. Aconitic acid is an intermediate metabolite in the tricarboxylic acid cycle. The decrease in its level in the model urine was a result of a functional disorder of mitochondria. Suberylglycine, an acyl glycine, is normally a minor metabolite of fatty acids. The decreased content in the model urine demonstrated that its metabolism was disordered, which was consistent with clinical reports of kidney yin deficiency. 5,6-Dihydrouridine is a pyrimidine that is the result of adding two hydrogen atoms to a uridine. Dihydrouridine is found only in tRNA molecules. The presence of 5,6-Dihydrouridine in the urine suggests an increased degradation rate of tRNA [22]. It has been reported that the urine degradation products of RNA vary significantly in some malignant tumor patients, so these metabolites are biomarkers of some cancers [23]. The main biological functions of tRNA are to transport the active amino acid and participate in the biosynthesis of proteins. The urine content of 5,6-dihydrouridine increased greatly in the model, indicating the degradation rate of tRNA was improved, which would affect the biosynthesis of proteins and the biological functions. Estrone is a major mammalian estrogen and can be detected in both blood and urine [24]. The serum content of E2 increased in the kidney yin deficiency model, which was consistent with the elevated level of estrone in the urine.

In the positive mode, 4,6-Dihydroxyquinoline was the most responsible ion for discrimination and is the product of the conversion of 5-hydroxykynurenamine by the enzyme monoamine oxidase, both metabolites from 5-hydroxytryptophan metabolism. 5-Hydroxytryptophan is a hormone secreted by the pars encephalica that can affect emotion, sleep and appetite of humans. 5-Hydroxytryptophan is also the precursor of 5-HT, an inhibitory substance of neural transmission. If the levels of 5-HT decrease, it can cause depression, anxiety and insomnia. In the present study, the content of 4,6-dihydroxyquinoline increased in the urine of the rat model, so the metabolism of 5-HT might be enhanced, which would affect neural regulation to induce changes in emotion. Creatinine is a breakdown product of creatine phosphate in muscle. The loss of a water molecule from creatine results in the formation of creatinine. Creatinine is transferred to the kidneys by blood plasma, whereupon it is eliminated from the body by glomerular filtration and partial tubular excretion. Creatinine is usually produced at a fairly constant rate by the body. Measuring serum creatinine is a simple test, and it is the most commonly used indicator of renal function. An increase in blood creatinine levels is observed only with marked damage to functioning nephrons [25,26]. It has been reported that thyroxine can affect kidney function, and on the other hand, kidney insufficiency can affect the action of thyroxine [27]. Accordingly after administration of thyroxine and reserpine, the urine content of creatinine increased greatly. However, to date there is no report about using urinary creatinine as an indicator to evaluate renal function. If urinary creatinine did have some relationship with renal function, it could alleviate patient distress

to some extent. L-Phenylalanyl-L-hydroxyproline is a proteolytic breakdown product of collagen. Collagen, a most structural protein, is an essential component of tissues, accounts for 25–33% of total proteins and 6% of body weight, and is a component of tissues and organs such as skeleton, ligaments and cornea. Collagen is the key component that maintains the modality of skin and tissues and is the raw material to repair the injured tissues. The catabolism of collagen is regulated by hormonal modulation, and hormone metabolic disorders induced by thyroxine and reserpine might lead to disturbances of collagen metabolism. Definitely, the urine content of L-phenylalanyl-L-hydroxyproline decreased significantly in the rat model. 3-Methylguanine is a methylated purine base. Methylated purine bases are known to be present in normal urine and to change under pathological conditions, in particular in the development of leukemia, tumors and immunodeficiency, by the altered turnover of nucleic acids typical of these diseases [28]. Thyroxine and reserpine lead to dysfunctions of the whole body, so the content of 3-methylguanine was greatly increased in the rat model. 3-Methoxytyrosine is one of the main biochemical markers for aromatic L-amino acid decarboxylase deficiency, an inborn error of metabolism that affects serotonin and dopamine biosynthesis. Patients are usually identified during infancy due to developmental delay, hypotonia and extrapyramidal movements. Diagnosis is based on an abnormal neurotransmitter metabolite profile in cerebrospinal fluid (CSF) and reduced aromatic L-amino acid decarboxylase (AADC) activity in plasma. 3-methoxytyrosine is elevated in CSF, plasma and urine [29]. After administration of thyroxine and reserpine, the urinary content of 3-methoxytyrosine increased significantly, which might be induced by disorders of substance and energy metabolism. 3-Methyldioxyindole and estrone were also detected in the negative mode, and the implications are as discussed previously.

All the results demonstrated that administration of thyroxine and reserpine disturbed the metabolic profile of healthy rats, and the 20 ions identified may be useful differentiating metabolites for the clinical diagnosis of kidney yin deficiency. After administration of LW, SB and SX, the metabolic profiles returned towards baseline to different extents, and LW-treated rats had the most similar metabolic profile to that of the control rats, indicating the greatest efficiency of the formula LW on the metabolomics level, which provides a novel method for evaluating formulas of Chinese medicine.

## 5. Conclusion

In the present study, a metabolomic approach based on the UPLC–HDMS technique and chemometrics method was employed to demonstrate the urinary metabolic characteristics induced by thyroxine and reserpine. Pattern recognition techniques such as PCA applied to the chromatographic data clearly identified the different groups. Twenty differentiating metabolites were preliminary identified using the OPLS analysis. Based on particular explanations of these ions, the relationship between differentiating metabolites and traditional bioinformatics was determined, which was also supported by blood biochemical examinations. These results suggest that metabolomics can connect the symptom pathogenesis of Chinese medicine with modern theory of medicine correctly, with differentiating metabolites as the proper link. With the development of databases and analytical techniques, the “material bases” of Chinese medicine symptoms may become more clear and may explain the scientific connotation of kidney yin deficiency. This approach may offer a powerful technique for symptom essence research in Chinese medicine, providing an experimental foundation for the clinical evaluation of kidney yin deficiency and a novel approach for the study of Chinese medicine formulas.

## Acknowledgment

The work was supported by grants from the Key Program of the Natural Science Foundation of State (China) (Grant NO. 30572300).

## References

- [1] J.K. Nicholson, J.C. Lindon, E.F. Holmes, Metabonomics understanding the metabolic responses of living systems to pathophysiological stimuli via multivariate statistical analysis of biological NMR spectroscopic data, *Xenobiotica* 29 (1999) 1181–1189.
- [2] X. Wang, H. Lv, H. Sun, L. Liu, B. Yang, W. Sun, P. Wang, D. Zhou, L. Zhao, S. Dou, G. Zhang, H. Cao, Metabolic urinary profiling of alcohol hepatotoxicity and intervention effects of Yin Chen Hao Tang in rats using ultra-performance liquid chromatography/electrospray ionization quadruple time-of-flight mass spectrometry, *J. Pharm. Biomed. Anal.* 48 (2008) 1161–1168.
- [3] E.M. Lenz, J. Bright, R. Knight, I.D. Wilson, H. Major, Cyclosporin A-induced changes in endogenous metabolites in rat urine: a metabonomic investigation using high field <sup>1</sup>H NMR spectroscopy, HPLC-TOF/MS and chemometrics, *J. Pharm. Biomed. Anal.* 35 (2004) 599–608.
- [4] J. Taylor, R.D. King, T. Altmann, O. Fiehn, Application of metabolomics to plant genotype discrimination using statistics and machine learning, *Bioinformatics* 2 (2002) 241–248.
- [5] B. Xu, J. Zhou, w. He, S. Lu, X. Kong, B. Shi, J. Huang, W. Li, Investigation on dexamethasone induced cleft palate in embryos of C57BL/6J mice by <sup>1</sup>H-NMR pattern recognition of metabolites group, *J. Biomed. Eng.* 16 (2009) 366–370.
- [6] K. Hiller, J. Hanqebrauk, C. Jaqer, J. Spura, K. Schreiber, D. Schomburg, Metabolite detector: comprehensive analysis tool for targeted and nontargeted GC/MS based metabolome analysis, *Anal. Chem.* 81 (2009) 3429–3439.
- [7] W. Lu, B.D. Bennett, J.D. Rabinowitz, Analytical strategies for LC-MS-based targeted metabolomics, *J. Chromatogr. B: Analyt. Technol. Biomed. Life Sci.* 87 (2008) 236–242.
- [8] P.A. Guy, I. Tavazzi, S.J. Bruce, Z. Ramadan, S. Kochhar, Global metabolic profiling analysis on human urine by UPLC-TOFMS: issues and method validation in nutritional metabolomics, *J. Chromatogr. B: Analyt. Technol. Biomed. Life Sci.* 871 (2008) 253–260.
- [9] W. Yin, et al., The effect of experimental hyperthyreosis on intestinal motility of rabbit in vitro, *J. Shanghai 1<sup>st</sup> Med. Col.* 4 (1957) 289.
- [10] C. Jiang, et al., Studies on kidney of Chinese traditional medicine (second edition), Shanghai Technol. Pub. Com, 1981.
- [11] A. Kuang, et al., Experimental studies on yin, yang of Chinese medicine (1), the effect of Radix Aconiti Lateralis Preparata, Cortex Cinnamomi Cassiae and Liu wei di huang wan on experimental hypertension, *J. Integrated tcm-wm.* 4 (1984) 742.
- [12] Physiology Group of Beijing Institute of Traditional Chinese Medicine. Initial studies on the reproduce of “deficiency zheng” model, Beijing Medical Society, Beijing Serial of Chinese Medical Theses, 1979, p. 82.
- [13] Y. Zhao, Y. Liu, Asymptomatic hyperuricemia and kidney injury, *J. Prac. Med.* 3 (2009).
- [14] S.A. Spindler, F.H. Sarkar, W.A. Sakr, M.L. Blackburn, A.W. Bull, M. LaGattuta, R.G. Reddy, Production of 13-hydroxyoctadecadienoic acid (13-HODE) by prostate tumors and cell lines, *Biochem. Biophys. Res. Commun.* 239 (1997).
- [15] J.T. Yen, B.J. Kerr, R.A. Easter, et al., Difference in rates of net portal absorption between crystalline and protein-bound lysine and threonine in growing pigs fed once daily, *J. Anim. Sci.* 82 (2004) 1079–1090.
- [16] S. Moehn, R.O. Ball, M.F. Fuller, et al., Growth potential but not bodyweight or moderate limitation of lysine intake, affects inevitable lysine catabolism in growing pigs, *J. Nutr.* 134 (2004) 287–292.
- [17] D. Behr-Roussel, A. Rupin, S. Simonent, et al., Effect of chronic treatment with the inducible nitric oxide synthase inhibitor N-*iminoethyl*-L-lysine or with L-arginine on progression of coronary and aortic atherosclerosis in hypercholesterolemic rabbits, *Circulation* 102 (2000) 1033–1038.
- [18] A. Olivieri, K. Tipton, J.O. Sullivan, L-lysine as a recognition molecule for the VAP-1 function of SSAO, *J. Neural. Transm.* 114 (2007) 747–749.
- [19] S. Hamilton, J. Odili, G.D. Wilson, et al., Reducing renal accumulation of single-chain Fv against melanoma-associated proteoglycan by coadministration of L-lysine, *Melanoma Res.* 12 (2000) 373–379.
- [20] W.L. Nyhan, Diagnostic Recognition of Genetic Disease Lea & Febiger, Philadelphia, 1987.
- [21] C. Guo, J. Gu, The effect of amine acid on immune system, *J. Ami. Acid* 5 (1988) 21–24.
- [22] H. Topp, R. Duden, G. Schoch, 5,6-Dihydrouridine: a marker ribonucleoside for determining whole body degradation rates of transfer RNA in man and rats, *Clin. Chim. Acta* 218 (1993) 73–82.
- [23] H.M. Liebich, C. Di Stefano, A. Wixforth, H.R. Schmid, Quantitation of urinary nucleosides by high-performance liquid chromatography, *J. Chromatogr. A* 763 (1997) 193–197.
- [24] M.E. Reichman, J.T. Judd, C. Longcope, A. Schatzkin, B.A. Clevidence, P.P. Nair, W.S. Campbell, P.R. Taylor, Effects of alcohol consumption on plasma and urinary hormone concentrations in premenopausal women, *J. Natl. Cancer Inst.* 85 (1993) 722–727.
- [25] T. Kikuchi, Y. Orita, A. Ando, H. Mikami, M. Fujii, A. Okada, H. Abe, Liquid-chromatographic determination of guanidino compounds in plasma and erythrocyte of normal persons and uremic patients, *Clin. Chem.* 27 (1981) 1899–1902.
- [26] A.D. Rule, T.S. Larson, E.J. Bergstralh, J.M. Slezak, S.J. Jacobsen, F.G. Cosio, Using serum creatinine to estimate glomerular filtration rate: accuracy in good health and in chronic kidney disease, *Ann. Intern. Med.* 141 (2004) 929–937.
- [27] U. Lebkowska, J. Malyszko, S. Brzosko, W. Lebkowski, J.S. Malyszko, J. Janica, R. Kowalewski, M. Gacko, M. Mysliwiec, J. Walecki, Renal artery resistance index, thyroid hormones, and thyroid volume in the early kidney transplants recipients, *Transplant Proc.* 38 (2006) 62–65.
- [28] B. Porcelli, L.F. Muraca, B. Frosi, E. Marinello, R. Vernillo, A. De Martino, S. Catinella, P. Traldi, Fast-atom bombardment mass spectrometry for mapping of endogenous methylated purine bases in urine extracts, *Rapid Commun. Mass Spectrom.* 11 (1997) 398–404.
- [29] I. Armando, E. Grossman, A. Hoffman, D.S. Goldstein, Method for measuring endogenous 3-O-methyl-dopa in urine and plasma, *J. Chromatogr.* 568 (1991) 45–54.